Journal of Colloid and Interface Science 474 (2016) 190–198

Contents lists available at ScienceDirect

Journal of Colloid and Interface Science

journal homepage: www.elsevier.com/locate/jcis

# Langmuir monolayers composed of single and double tail sulfobetaine lipids

Gavin Hazell [a], Anthony P. Gee [a], Thomas Arnold [b], Karen J. Edler [a,*], Simon E. Lewis [a]

[a] Department of Chemistry, University of Bath, Claverton Down, Bath BA2 7AY, UK
[b] Diamond Light Source, Harwell Science and Innovation Campus, Didcot OX11 0DE, UK

## GRAPHICAL ABSTRACT

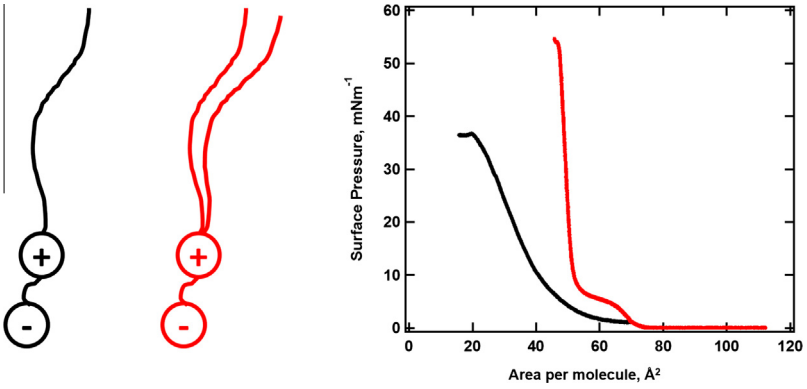


## ARTICLE INFO

*Article history:*
Received 3 February 2016
Revised 13 April 2016
Accepted 14 April 2016
Available online 26 April 2016

*Keywords:*
Sulfobetaine
Lipids
Langmuir monolayers
Reflectometry
Air-water interface

## ABSTRACT

*Hypothesis:* Owing to structural similarities between sulfobetaine lipids and phospholipids it should be possible to form stable Langmuir monolayers from long tail sulfobetaines. By modification of the density of lipid tail group (number of carbon chains) it should also be possible to modulate the two-dimensional phase behaviour of these lipids and thereby compare with that of equivalent phospholipids. Potentially this could enable the use of such lipids for the wide array of applications that currently use phospholipids. The benefit of using sulfobetaine lipids is that they can be synthesised by a one-step reaction from cheap and readily available starting materials and will degrade via different pathways than natural lipids. The molecular architecture of the lipid can be easily modified allowing the design of lipids for specific purposes. In addition the reversal of the charge within the sulfobetaine head group relative to the charge orientation in phospholipids may modify behaviour and thereby allow for novel uses of these surfactants.
*Experiments:* Stable Langmuir monolayers were formed composed of single and double tailed sulfobetaine lipids. Surface pressure-area isotherm, Brewster Angle Microscopy and X-ray and neutron reflectometry measurements were conducted to measure the two-dimensional phase behaviour and out-of-plane structure of the monolayers as a function of molecular area.
*Findings:* Sulfobetaine lipids are able to form stable Langmuir monolayers with two dimensional phase behaviour analogous to that seen for the well-studied phospholipids. Changing the number of carbon tail groups on the lipid from one to two promotes the existence of a liquid condensed phase due to increased

* Corresponding author.
*E-mail address:* k.edler@bath.ac.uk (K.J. Edler).

http://dx.doi.org/10.1016/j.jcis.2016.04.020

Van der Waals interactions between the tail groups. Thus the structure of the monolayers appears to be defined by the relative sizes of the head and tail groups in a predictable way. However, the presence of sub-phase ions has little effect on the monolayer structure, behaviour that is surprisingly different to that seen for phospholipids.


## 1. Introduction

Sulfobetaine amphiphiles are zwitterionic species of interest for a vast array of applications. They are used industrially to stabilize foams against the anti-foaming properties of oil droplets found in shampoo and conditioners [1]. With both positively and negatively charged regions in their head groups, they are non-toxic and not harmful to the skin and eyes [2]. As such they have been shown to enhance the biocompatibility of systems that will need to interact with biological fluids (e.g. polymers [3], medical implants [4] and biosensors [5,6]). One such recent publication has demonstrated their application in temperature-responsive drug release [7]. In addition, they are stable in hard water and resistant to oxidation, a considerable advantage over some other surfactants. It has also been demonstrated that large changes in pH and temperature do not have detrimental effects on these desirable properties [8].

Their structure comprises an inner quaternary ammonium ion, linked to an outer sulfonate by a hydrocarbon linker group (Fig. 1). When the tails are sufficiently long these amphiphiles are structurally similar to many phospholipids (particularly phosphocholine (PC) based lipids), but importantly with the opposite charge distribution in their head groups (see Fig. 1). However, in contrast to phospholipids that are expensive to produce and require lengthy, multi-step synthetic procedures, sulfobetaine lipids can be made using a one-step reaction from cheap starting materials [8,9]. These materials can therefore be more easily tailored to specific applications. Changes in tail group length, density and structure are straightforward, as well as modification of the linker length between charged moieties in the head group [8]. This makes their synthesis easier, more flexible and more economically effective compared to phospholipids. Given these added advantages it is important that the physicochemical properties of this class of lipid are investigated in order to utilise them to their full potential.

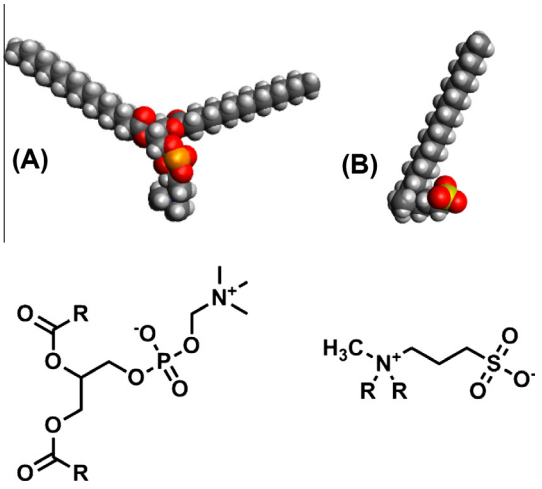


**Fig. 1.** Space filling (Dark Grey = Carbon, Light Grey = Hydrogen, Red = Oxygen, Blue = Nitrogen, Yellow = Sulphur and Orange = Phosphorous) structures of lipid molecules and molecular structures of the head groups of (A) a phosphocholine lipid and (B) sulfobetaine lipid.

It is already known that phospholipids are capable of forming an array of structures both in solution (vesicles [10], lamellar phases [11]) and at air-water [12], oil-water [13] and solid-water interfaces [14]. One area which has received particular attention is their ability to form highly stable Langmuir monolayers. These monolayers can be transferred to solid interfaces by well-established techniques [15,16] and find uses in protein alignment [17], biosensing [18] and biocompatible coatings [19]. When spread at the air-water interface phospholipids exhibit two-dimensional phase transitions as a function of molecular area [20]. Interestingly the surface pressure at the onset of these phase transitions is responsive to the presence of several types of salt in the water sub-phase [21]. The presence of salt also has important effects for the transfer to solid interfaces [22] and the interaction with proteins [23]. Given the similarity in structure between phospholipids and sulfobetaines it is expected that sulfobetaines will be capable of forming stable Langmuir monolayers which could then be appropriate to the same kinds of applications already mentioned for phospholipids. It is also important to assess whether the presence of salt has structural effects on sulfobetaine monolayer properties, as with their phospholipid counterparts, where added salt alters the position of the phase plateau onset. However, despite this large number of potential applications and the fact that they are already commonly used commercially, their physicochemical properties have received far less attention than their phospholipid counterparts.

Here we report an investigation into the Langmuir films of two sulfobetaine lipids at the air-water interface. The lipids have been chosen to be analogues of single tailed and double tailed phospholipids, so that we can make a direct comparison to the well-known behaviour of those systems. We have used Brewster angle microscopy (BAM), X-ray/neutron reflectometry (XRR/NR) and Langmuir trough techniques to obtain new structural information about these lipids that will inform our future studies.

## 2. Experimental

### 2.1. Materials

In this study we have investigated two sulfobetaines, one with a single alkyl tail and the other with two alkyl chains. For convenience we will hereafter refer to these compounds with the following notation: SBx-y-z, where x is the number of carbons in the head group linker, y is the number of carbons in the alkyl tail and z is the number of tails (only listed for z > 1). The full names for the compounds used here are *3-(dimethyloctadecylammonio)propane-1-sulfonate* (hereafter referred to as SB3-18) and *3-(methyldioctadecylammonio)propane-1-sulfonate* (hereafter referred to as SB3-18-2).

Where possible, we have purchased chemicals: NaCl, $CaCl_2$, SB3-18, 1,3-propanesultone, dimethylamine were purchased from Sigma-Aldrich at purity levels of 96% or higher. The deuterated SB3-18 and hydrogenated SB3-18-2 were synthesised. Full procedures and characterisation of the resulting materials can be found in the supplementary material. The key chemicals for this synthesis, Bromooctadecane-$d_{37}$ (98% purity and 98% deuteration) and

*N*-methyl-*N*-octadecyloctadecan-1-amine (95% purity) were purchased from CDN isotopes (Quebec, Canada) and ABCR Chemicals (Germany) respectively. All chemicals were used without further purification. Deionized water was purified with a Mili-Q Plus (Milipore, Schwalbach, Germany) to achieve a resistivity of 18 MΩ cm.

### 2.2. Methods

#### 2.2.1. Langmuir trough studies

Monolayers of the insoluble lipids were prepared by the deposition of a 100 µl solution (0.5 mg ml$^{-1}$ in chloroform) over the sub-phase. Ten minutes was allowed for chloroform evaporation and monolayer equilibration. Surface pressure - Area (π-A) isotherm measurements were carried out using a Nima Langmuir type 611 trough, using a 1 cm wide Wilhelmy plate sensor. All salt subphases used were at a concentration of 50 mM to ensure sufficient interaction of ions with the lipid head groups. π-A isotherm measurements were conducted using a double-barrier compression system at a compression rate of 20 cm$^2$ min$^{-1}$ to ensure high resolution in the resulting isotherms. Other compression speeds were trialled but made no discernable difference to the shape of the isotherm. Therefore a compression rate of 20 cm$^2$ min$^{-1}$ has been used for all data presented here. All the isotherms reported in this paper are the averages of at least three experiments.

#### 2.2.2. Brewster angle microscopy

BAM was used to observe domain formation within the monolayer films. The theory of BAM measurements is described in detail elsewhere [24,25] and experiments reported here were conducted using a Nanofilm EP3 imaging ellipsometer (532 nm). Monolayers were prepared as above on a purpose made Nima 712BAM trough. The BAM images were recorded periodically throughout continuous compression (at the same rate as above).

#### 2.2.3. Reflectometry

The specular reflection of neutrons and X-rays is measured as a function of the scattering vector, Q, which lies perpendicular to the surface normal ($Q = 4\pi \sin\theta/\lambda$), where $\theta$ is the angle of incidence and $\lambda$ is the wavelength of the neutron or X-ray beam [26]. The experimental reflectivity is therefore related to the square of the Fourier transform of the scattering length density (SLD) distribution, $\rho(z)$, normal to the surface. For neutrons $\rho(z) = \sum_i n_i(z) \cdot b_i$, where $n_i$ and $b_i$ are the number density and scattering length of the ith component and z is the direction perpendicular to the surface [27]. For X-rays $\rho(z)$ is found by replacing $b_i$ with $Zr_e$ where $r_e$ is the classical radius of an electron and $Z$ is the atomic number of the ith component [28]. The reflectivity can therefore be expressed as,

$$R(Q) = \frac{16\pi^2}{Q^2}\left|\int \rho(Z)e^{-iQz}\right|^2$$

In the case of neutrons $\rho(z)$ can be modified by deuterium labelling (H and D have very different scattering lengths, $-3.74 \times 10^{-6}$ Å for H and $6.67 \times 10^{-6}$ Å for D [29]), which means that multiple neutron "contrasts" can be obtained for the same system and can thereby provide detailed information about structure of an adsorbed layer [30]. However, low flux and high background scattering limit the maximum Q that is accessible using neutrons. For X-ray reflectivity, although contrast variation is not possible, the photon flux at a synchrotron source is several orders of magnitude higher and the background scattering is significantly reduced relative to neutron sources. These are therefore highly complementary techniques that can be exploited to provide both high resolution and a highly constrained model to explain the surface structure for a wide range of surfactant and lipid systems [26,31–36].

XRR measurements presented here were conducted using beamline I07 at Diamond Light Source (Oxford, U.K.) using the "double crystal deflector" (DCD) for reflectivity from liquid interfaces [37] at 12.5 keV. Data was collected using a region of interest on a Pilatus 100k detector to integrate the specular reflection, whilst a second region of interest of the same size was used to approximately subtract the background. A "footprint" correction [38] for over-illumination was applied to the data assuming a Gaussian beam profile and ignoring meniscus effects. The data was collected over three attenuation regimes and normalized to the critical edge. In order to minimize beam damage the trough was enclosed under a helium atmosphere and horizontally translated by small increments between each attenuation regime.

NR measurements [39] were conducted using the INTER beamline [40] on Target Station 2 and the SURF beamline [41] on Target Station 1 at the ISIS Pulsed Neutron Source (Oxford, U.K). Measurements used a single point detector and fixed grazing incidence angles (0.8° and 2.3° on INTER and 1.5° SURF). The absolute reflectivity was calibrated with respect to the direct beam and the reflectivity from a clean $D_2O$ surface.

Two different contrasts were obtained from the NR experiments. For the single tailed lipid hydrogenated SB3-18 was measured on $D_2O$ and deuterated SB3-18 was measured on air contrast matched water (ACMW; 8 mol% $D_2O$ in $H_2O$ with an SLD of 0). We were unable to deuterate the double tailed lipid so hydrogenated SB3-18-2 was measured on 100% $D_2O$ and 70% by volume $D_2O$ in $H_2O$ to ensure that two isotopic contrasts were obtained. In both cases these were combined with the additional X-ray contrast and fitted simultaneously using MOTOFIT, written for IGOR Pro [42]. MOTOFIT uses the Abeles matrix [43,44] method to calculate the reflectivity profile from a scattering length density profile for a model composed of layers each with a thickness, t, a scattering length density, SLD, and a term for the roughness between layers, σ.

In each of these experiments the surface pressure of the monolayer was controlled with a Nima trough (20 × 40 cm). For the single tailed lipid, measurements were made at surface pressures of 15, 20 and 25 mN m$^{-1}$ and for the double tailed lipids at 6 and 35 mN m$^{-1}$. Since X-ray and neutron beamtime is limited, different surface pressures for SB3-18-2 compared to SB3-18 were chosen, so that measurements could be taken within the phase transition plateau and the liquid condensed domain. As SB3-18 shows no phase transition, its structure was measured at three evenly spaced points throughout its compression isotherm. The stability of the surface pressure during measurement was ±3 mN m$^{-1}$ (approximately ±15%). The time taken for each measurement was ~15 min for XRR and 30 min for NR. This variability has introduced an error in the area per molecule (APM), which has implications for the constraints applied to subsequent reflectometry fitting (see below).

In order to constrain our fits to the reflectometry data we have accepted only fits that are consistent with the APM determined from our isotherm data for the surface pressure in question. The modeled APM value is obtained from the theoretical scattering length of the (part)molecule and dividing it by the product of the thickness and SLD of the entire layer. This calculated APM was constrained to ensure that it was within 10% of the value obtained from isotherm data. We believe this 10% limit is reasonable because of a number of factors; including the static versus dynamic nature of the two experiments and the repeatability of the measurement from one contrast to the next [45]. Table 1 compares the experimental isotherm APM with the values calculated from the models described in Tables 2 and 3.

**Table 1**
Comparison between APM values determined from experimental isotherm measurements and extracted from the models used to simulate the X-ray & Neutron data. (–) denotes no percentage difference as the values for the isotherm and modeled APMs match within their uncertainties.

| | Surface pressure/ mN m$^{-1}$ | Isotherm APM/Å$^2$ | Modeled APM/Å$^2$ | Percentage difference |
|---|---|---|---|---|
| SB3-18 | 15 | 36 ± 1 | 35 ± 1 | (–) |
| | 20 | 32 ± 2 | 34 ± 1 | (–) |
| | 25 | 30 ± 1 | 33 ± 1 | +9.8% |
| SB3-18-2 | 6 | 64 ± 1 | 69 ± 1 | +8.6% |
| | 35 | 38 ± 1 | 35 ± 1 | −8.1% |

## 3. Results

### 3.1. Surface pressure-area isotherms and Brewster angle microscopy

The π-A isotherms of SB3-18 and SB3-18-2 on water are shown in Fig. 2. For SB3-18 the rise in surface pressure is monotonic until the monolayer collapses at 37 ± 1 mN m$^{-1}$ and 20 ± 1 Å$^2$ per molecule. In contrast the rise in surface pressure for SB3-18-2 is not monotonic, showing a plateau in the surface pressure before rising sharply to a maximum surface pressure of around 54 ± 3 mN m$^{-1}$ and 38 ± 1 Å$^2$. By analogy to the behaviour of double-tailed phospholipids we expect that this plateau is characteristic of a phase transition, which begins at 4.3 mN m$^{-1}$ (±0.6 mN m$^{-1}$) and 60.1 Å$^2$ (±0.7 Å$^2$).

Also shown in Fig. 2 is the surface compressional modulus, $C_S$, vs. surface pressure for the monolayer (defined as $C_S^{-1} = Ad\pi/dA$). This parameter is a useful guide to the physical state of a lipid within a monolayer, tending toward higher values for condensed monolayers [46,47]; typically surfactants found in the LC (Liquid-Condensed) phase exhibit values between 80 and 100 mN m$^{-1}$ [48]. For SB3-18, the isotherm suggests that the monolayer remains in a LE (Liquid-Expanded) state throughout lateral compression since there is no phase plateau and the maximum surface compressional modulus of 52 mN m$^{-1}$ lies within the regime of a film with LE character laid out by Davies and Rideal [48,49]. Meanwhile the maximum of the surface compressional modulus for SB3-18-2 is 184 mN m$^{-1}$ a value that is well into the LC regime [49] and is very similar to values reported for double tailed phospholipids (around ~200 mN m$^{-1}$) [50,51].

For SB3-18 BAM images are completely homogenous, showing no domain formation (see supplementary information). The BAM images show a smooth and homogenous film throughout lateral compression (15–25 mN m$^{-1}$). This is similar to the behaviour for single tailed lipids and is in agreement with that reported for single tailed phospholipids [48,52,53]. As suggested above, we expect that the phase plateau seen in SB3-18-2 isotherms corresponds to the lipid entering a phase co-existence region. Fig. 3 shows BAM images taken during an isotherm in this plateau region. The images show some domains that begin to nucleate at the onset of this plateau. These domains grow in a dendritic manner, until at higher surface pressures they begin to interact with one another, converge and form a liquid condensed film. The LC film is shown in Fig. 3 at a surface pressure of 35 mN m$^{-1}$. Such behaviour is characteristic of non-equilibrium growth of domains in lipid systems as observed by BAM [25].

The influence of sub-phase salt solutions were also studied. Measurements were conducted for several sub-phases containing

**Table 2**
Fit parameters for SB3-18 monolayer on three different sub-phases at surface pressures of 15, 20 and 25 mN m$^{-1}$.

| Layer | Scattering length density/ $10^{-6}$ Å$^{-2}$[a] | | | Sub-phase | Model: Surface pressure/mN m$^{-1}$ | | | | | | | | |
|---|---|---|---|---|---|---|---|---|---|---|---|---|---|
| | | | | | 15 | | | 20 | | | 25 | | |
| | $D_2O$ | ACMW | X-ray | | t/Å | σ/Å | % Hyd | t/Å | σ/Å | % Hyd | t/Å | σ/Å | % Hyd |
| SB3-18 Tail[b] | −0.36 | 7.2 | 7.9 | Water | 8.6 ± 0.3 | 3.7 ± 0.1 | | 8.8 ± 0.2 | 4.6 ± 0.3 | | 9.5 ± 0.3 | 5 ± 0.2 | |
| | | | | NaCl | 8.6 ± 0.3 | 3.4 ± 0.2 | | 8.7 ± 0.4 | 4.7 ± 0.1 | | 9.8 ± 0.2 | 4.9 ± 0.2 | |
| | | | | $CaCl_2$ | 8.5 ± 0.2 | 3.5 ± 0.3 | | 8.8 ± 0.3 | 4.6 ± 0.2 | | 9.6 ± 0.3 | 5 ± 0.2 | |
| SB3-18 Head | 0.99 | | 14.4 | Water | 4.9 ± 0.4 | 3.7 ± 0.2 | 55 ± 3 | 4.9 ± 0.2 | 3.2 ± 0.2 | 44 ± 4 | 4.9 ± 0.3 | 3.7 ± 0.2 | 33 ± 5 |
| | | | | NaCl | 4.9 ± 0.4 | 3.8 ± 0.1 | 48 ± 6 | 5.0 ± 0.3 | 3.2 ± 0.2 | 40 ± 6 | 4.9 ± 0.2 | 3.6 ± 0.2 | 34 ± 4 |
| | | | | $CaCl_2$ | 4.9 ± 0.3 | 3.2 ± 0.1 | 60 ± 3 | 4.7 ± 0.4 | 3.0 ± 0.2 | 43 ± 3 | 4.9 ± 0.3 | 3.5 ± 0.2 | 35 ± 4 |
| Water | 6.35 | 0 | 9.45 | | | 3.2 ± 0.3 | | | 3.2 ± 0.2 | | | 3.8 ± 0.3 | |

[a] The SLD of the tail group was calculated assuming a molecular tail group volume of 510 Å$^3$, previously calculated for a cationic surfactant with a similar alkyl tail length [32], whilst the SLD of the head group was calculated assuming a volume of 181 Å$^3$, derived from characterisation of sulfobetaine micelles [60].
[b] Deuterated tail used on ACMW, hydrogenated tail used on $D_2O$.

**Table 3**
Fit parameters for SB3-18-2 monolayer at surface pressures of 6 and 35 mN m$^{-1}$.

| Layer | Scattering length density/ $10^{-6}$ Å$^{-2}$[a] | | | Subphase | Model: Surface pressure/mN m$^{-1}$ | | | | | |
|---|---|---|---|---|---|---|---|---|---|---|
| | | | | | 6 | | | 35 | | |
| | $D_2O$ | 70% $D_2O$ | X-ray | | t/Å | σ/Å | % Hyd | t/Å | σ/Å | % Hyd |
| SB3-18-2 Tail | −0.46 | | 9.1 | Water | 6.8 ± 0.4 | 5.1 ± 0.3 | | 17.8 ± 0.3 | 4.6 ± 0.5 | |
| | | | | NaCl | 8.0 ± 0.4 | 5.5 ± 0.3 | | 18 ± 0.3 | 5.3 ± 0.2 | |
| | | | | $CaCl_2$ | 7.3 ± 0.4 | 5.2 ± 0.5 | | 18.4 ± 0.2 | 5.0 ± 0.2 | |
| SB3-18-2 Head | 0.99 | | 14.4 | Water | 5.6 ± 0.3 | 3.0 ± 0.5 | 61 ± 4 | 6.8 ± 0.4 | 3.1 ± 0.3 | 39 ± 5 |
| | | | | NaCl | 4.9 ± 0.3 | 2.8 ± 0.2 | 48 ± 3 | 4.8 ± 0.3 | 3.5 ± 0.2 | 37 ± 3 |
| | | | | $CaCl_2$ | 4.9 ± 0.4 | 2.9 ± 0.4 | 47 ± 4 | 4.7 ± 0.4 | 3.4 ± 0.2 | 42 ± 5 |
| Water | 6.35 | 4.28 | 9.45 | | 3.0 ± 0.4 | | | 3.2 ± 0.3 | | |

[a] The SLD of the head group used was the same as SB3-18 (see Table 2). The scattering length density of the tail group was taken as a value previously been reported for a cationic surfactant with the same tail structure [61].

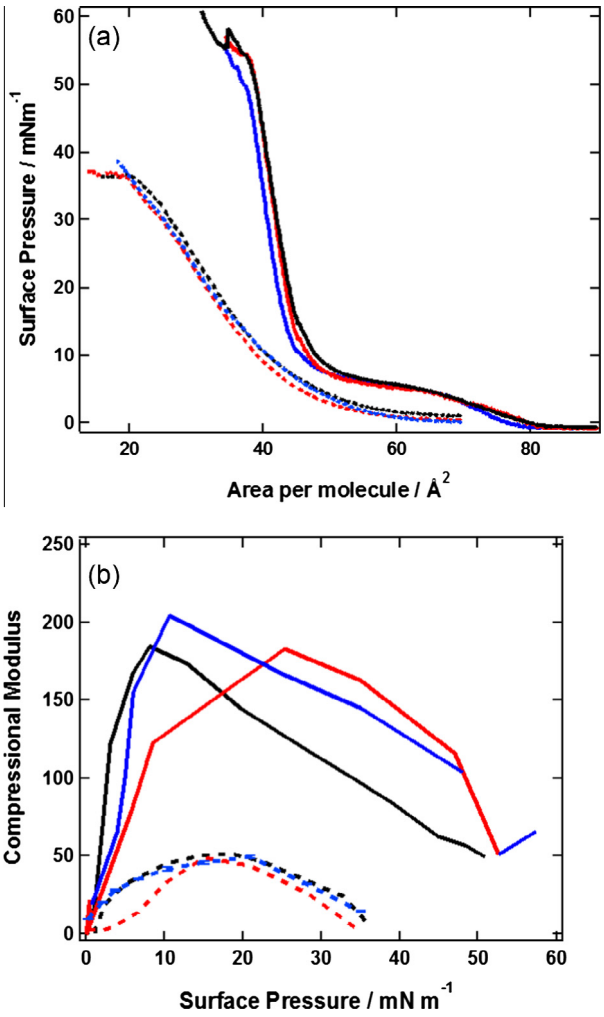


**Fig. 2.** (a) Pressure-Area (π-A) isotherms and b) surface compressional modulus for SB3-18 (dashed lines) and SB3-18-2 (solid lines) on pure water (black), NaCl (red) and $CaCl_2$ (blue). (For interpretation of the references to colour in this figure legend, the reader is referred to the web version of this article.)

50 mM salts, including NaCl, $CaCl_2$, NaBr, $ZnCl_2$, $BaCl_2$, $MgCl_2$ and $CsCl_2$. To illustrate these results we have included data for NaCl and $CaCl_2$ in Fig. 2, but the results for the other salts listed above are all very similar. With the exception of a small decrease in APM for any fixed surface pressure, the presence of salt in the sub-phase has very little effect on these isotherms for both SB3-18 and SB3-18-2. Such behaviour is not inconsistent with a diffuse ion layer beneath the surfactant head groups but importantly it does suggest there is no significant ion penetration into the head group region. This is in marked contrast to certain phospholipids where significant ion penetration has been observed [54,55]. In isotherms such behaviour is evident by an increase in APM at fixed surface pressures and is particularly notable for $Ca^{2+}$ ions [21].

### 3.2. X-ray and neutron reflectometry

Figs. 4 and 5 show a set of co-refined XRR and NR data with corresponding SLD profiles for SB3-18 and SB3-18-2 respectively. We have summarized the key findings in Fig. 6 whilst the structural parameters for the models used to calculate these fits are detailed in Tables 2 and 3. The left hand side of each table details the SLD for each layer of the proposed model; lipid tail, lipid head and sub-phase. These values were calculated as described earlier, using standard methods. We have chosen these values as our best estimate, and the subsequent fitting parameters are critically dependent on this choice. The right hand side of the tables gives structural parameters for each of these layers at defined surface pressures. These structural parameters are layer thickness (Å), layer roughness (Å) and percentage hydration (% volume fraction of water). For SB3-18 we see a change in thickness of the monolayer as the lipid is laterally compressed. The overall thickness increases by only a small amount (around 1 Å: 13.5 ± 0.3 Å to 14.4 ± 0.3 Å) over the surface pressure range measured (15–25 mN $m^{-1}$). This behaviour is consistent with that expected for a single chained surfactant found in the LE phase [48,53,56]. This is in contrast to the double chained lipid, SB3-18-2, where the effect of lateral compression is much more pronounced. In this case the thickness of the monolayer increases by around 11 Å (from 11.6 ± 0.5 Å at 6 mN $m^{-1}$ to 22.6 ± 0.7 Å at 35 mN $m^{-1}$). This is consistent with what we would expect from this system based on the isotherm and BAM data presented above. At 6 mN $m^{-1}$ the monolayer remains in the phase co-existence (LE-LC) region so is expected to exhibit a thickness comparable to the single tailed lipid. At 35 mN $m^{-1}$ the monolayer is in the LC phase with a corresponding increase in thickness. This is consistent with the behaviour seen for double tailed phospholipids [50,57–59] and can be explained by an increase in alkyl tail volume with a corresponding increase in the number of Van der Waals interactions compared to the single tail case.

XRR and NR experiments were also performed on NaCl and $CaCl_2$ sub-phases. As with the isotherm data, no discernible difference was observed between the pure water and salt sub-phases. The details of the fits for this data are included in Tables 2 and 3.

## 4. Discussion

Table 4 shows some physical parameters derived from the Langmuir isotherm data presented in Fig. 2 for SB3-18 and SB3-18-2, together with literature values for some structurally

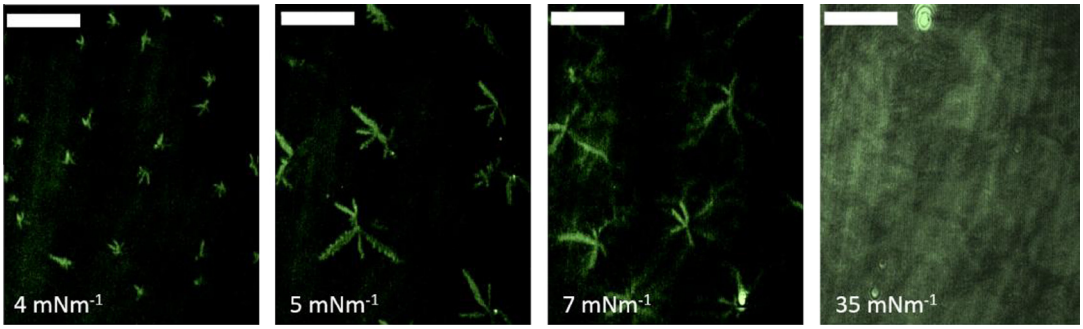


**Fig. 3.** BAM images for SB3-18-2 on water at surface pressures throughout the LE-LC transition; the plateau region of the isotherm shown in Fig. 2. The scale bar represents 50 μm.

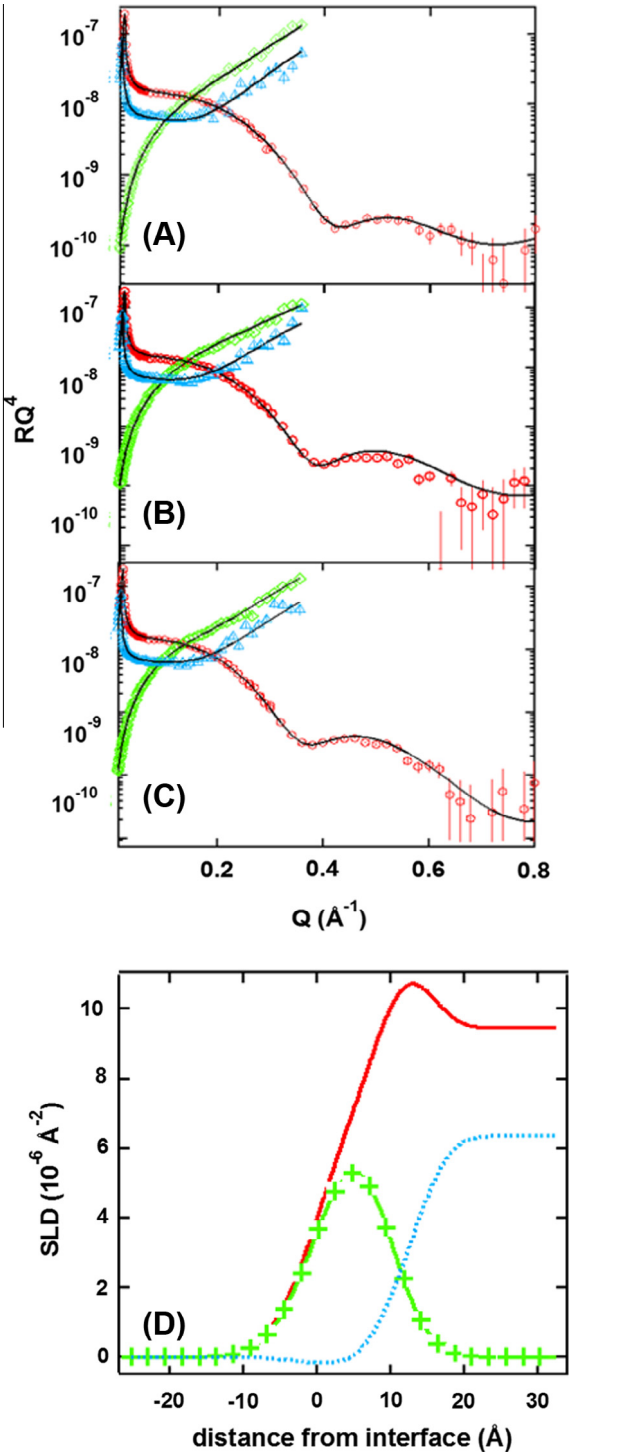


**Fig. 4.** XRR and NR data for SB3-18 at (A) 15, (B) 20 and (C) 25 mN m$^{-1}$ along with (D) an example SLD profile at 25 mN m$^{-1}$. In the reflectometry curves (A–C) X-ray data is shown in red circles, deuterated SB3-18 neutron data on ACMW in green diamonds and hydrogenated SB3-18 neutron data on $D_2O$ in blue triangles. The black line represents the model fit to the data. In the SLD profile (D) X-ray data is shown as solid red line, deuterated SB3-18 neutron data on ACMW is shown as green line with crosses and hydrogenated SB3-18 data on $D_2O$ is shown as dashed blue line. (For interpretation of the references to colour in this figure legend, the reader is referred to the web version of this article.)

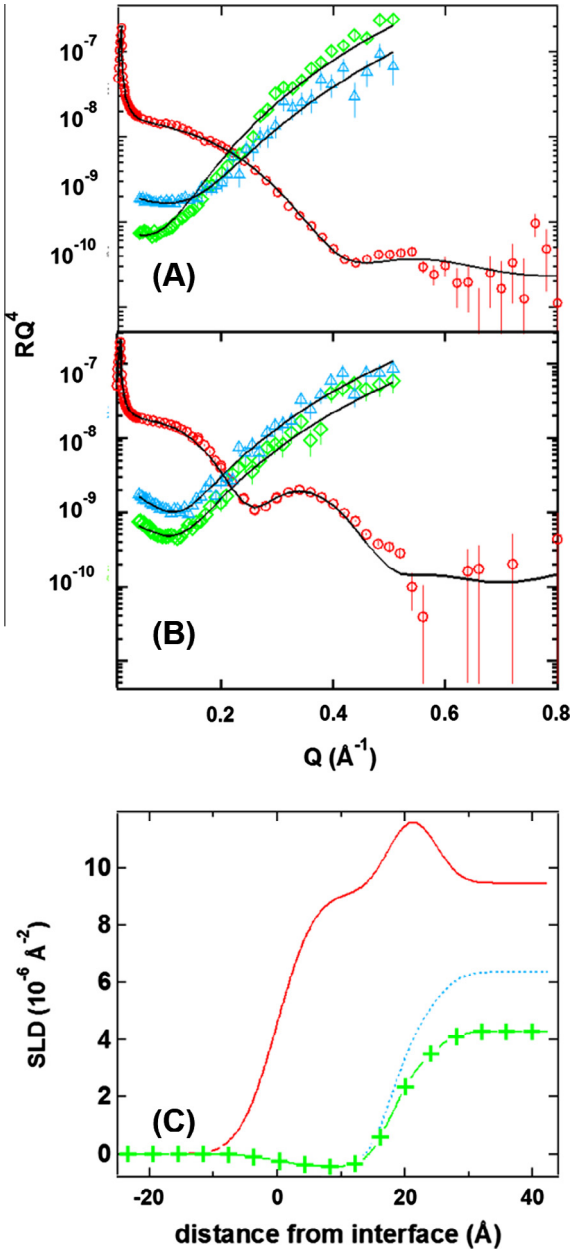


**Fig. 5.** XRR and NR data for SB3-18-2 at (A) 6 and (B) 35 mN m$^{-1}$ along with (C) an example SLD profile at 35 mN m$^{-1}$. In the reflectometry profiles (A and B) X-ray data is shown in red circles, hydrogenated SB3-18-2 on $D_2O$ in blue triangles and hydrogenated SB3-18-2 on 70% $D_2O$ in $H_2O$ in green diamonds. The black line represents the model fit to the data. In the SLD profile (C) X-ray data is shown in solid red line, hydrogenated SB3-18-2 on $D_2O$ as blue dashed line and hydrogenated SB3-18-2 on 70% $D_2O$ in $H_2O$ as green line with crosses. (For interpretation of the references to colour in this figure legend, the reader is referred to the web version of this article.)

equivalent phospholipids 1-stearoyl-2-hydroxy-sn-glycero-3-phos phocholine ($C_{18}$Lyso-PC) and 1,2-dipalmitoyl-sn-glycero-3-phos phocholine (DPPC) respectively. The values of compressional modulus ($C_s^{-1}$) and the surface pressure at the collapse point ($\pi_{col}$) are comparable between the sulfobetaines studied here and their equivalent phospholipids [48,50,52,53,57], and in both cases the modulus is fractionally higher for the phospholipid. The area occupied by one molecule at various points in the isotherms does, however, reveal some more substantial differences between these lipid types. The collapse point ($A_{lim}$) and the area of collapse ($A_{col}$) are lower for sulfobetaines. These values can be understood by considering the difference in size of the headgroups. The phosphocholine (PC) headgroup is considerably larger than the sulfobetaine headgroup (see Fig. 1). The values found for the PC type lipids are characteristic of bulky headgroups bound to tails with a low cross

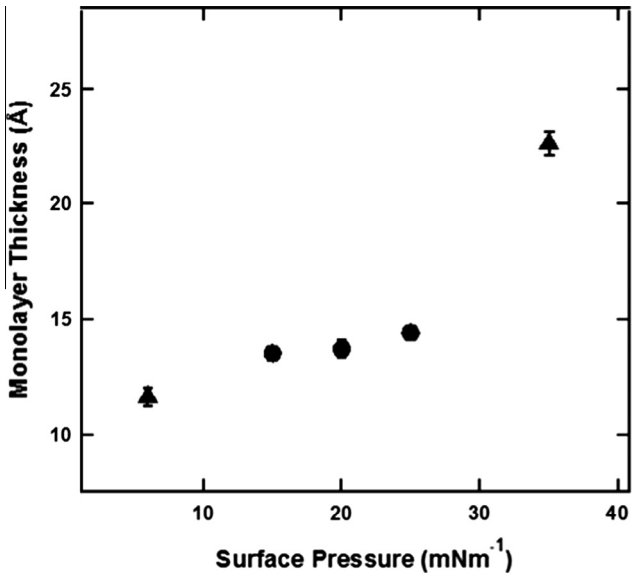


**Fig. 6.** Variation in chain thickness with increasing surface pressure for SB3-18 (circles) and SB3-18-2 (triangles).

sectional area [53]. Such a large headgroup relative to the area occupied by the tail group is expected to impede packing of molecules and leads to larger values of $A_{lim}$ and $A_{col}$ [62].

As the surface pressure rises, the reflectometry data shows that the thickness of the tail group does not increase significantly for the single tailed SB3-18 but does for the double tailed SB3-18-2 (Fig. 6). This shows that as the SB3-18-2 monolayer is compressed the alkyl tails are pushed away from the surface to a greater extent than for SB3-18. A simple trigonometric calculation based on the theoretical length of an all-trans 18-carbon tail (22.8 Å) and the observed thickness of the monolayer can be used to estimate this tilt angle. Such calculated values for the sulfobetaines measured here are included in Table 4. Over the surface pressure ranges studied, the chain tilt angle of SB3-18 only changes by about 2° (from 54° to 52° relative to the surface normal) but for SB3-18-2 the change is over 50° (from 59° to 8° relative to the surface normal). This phenomenon is well documented for PC lipid monolayers analysed by means of reflectometry [48,53,63], and is a direct result of an increased number of Van der Waals interactions for the double tail case.

It is notable that the tilt angles of the sulfobetaines are substantially lower (i.e. the tails stand up more vertically) than the structurally analogous PC-phospholipids [20,48] (see Table 4). We believe that this is because of the difference in the relative sizes of the head and tail groups for these two types of molecule. The PC headgroup is larger than the SB headgroup which relatively speaking hinders the close approach of the PC head groups. This therefore allows a greater area per molecule for a given surface pressure for the PC lipids and means that the tail packing is not as restricted as it is for the sulfobetaines. Consequently the chain tilt values are larger for PC lipids [52] (i.e. the PC lipid molecules lie flatter on the water surface).

## 5. Conclusion

Owing to structural similarities between sulfobetaine lipids and phospholipids, stable Langmuir monolayers composed of two different sulfobetaine surfactants have been formed. Monolayers have been structurally characterised and reveal behaviour that is similar to that seen for equivalent phospholipids, but with some important differences [64]. The packing of the lipids within the monolayer is modified as expected based on consideration of the relative size of the head and tail groups. This means that the sulfobetaines can be expected to behave in predictable ways relative to the behaviour of similar, well-studied phospholipids [50]. However, importantly the presence of simple metal salts (NaCl and $CaCl_2$) in the sub-phase does not significantly alter the structure or two-dimensional phase behaviour of these lipids. This is important because this is not the case for phospholipids, which show significant interactions with sub-phase cations [21]. This difference is a little surprising if we consider the relative charge distribution within the respective head groups. For phospholipids, the negative charge is buried away from the sub-phase within the head group. Any interaction with cations must therefore involve the cations being drawn into the head group beyond the unfavourable interaction with the positive charge in the outer head group. For sulfobetaines this charge distribution is reversed and so we might expect a more significant interaction between the cations and the negative charge in the outer head group. This is not the case and any interaction is found to have a very limited effect on the structure and behaviour of the sulfobetaine monolayers. We also note that experiments with a variety of subphase anions showed similarly limited effects on sulfobetaine monolayer behaviour. This means that the interaction between the sulfobetaine headgroup and ions in solution is diffuse in nature and does not influence interactions between neighbouring sulfobetaines. This may have advantages in applications of these species in high salt environments, or where the nature or type of ions which may be encountered is unpredictable.

Until now, very little was known about the behaviour of sulfobetaine lipids despite a wide array of applications. This study has shown that these systems have a number of desirable properties such as being able to form monolayers with well-pronounced phase behaviour, so that molecular coverage and physical state could be easily manipulated by synthetically controlling the molecular architecture. They are also capable of maintaining that structure in the presence of relatively high salt concentrations with no observed ion specific adsorption, a feature that is attractive for their potential use in vivo. The fact that they behave in a similar manner to the phospholipids makes them appealing candidates for other techniques that have been developed with phospholipids [13,17,65]. For example they have the potential to be transferred to the solid-liquid interface perhaps using vesicle fusion methods. This could enable uses in technological applications such as medical implants, drug delivery and biosensing membranes. This offers

**Table 4**
Physical parameters derived from π-A isotherms and reflectometry data for SB3-18 and SB3-18-2 as well as parameters from the literature for structurally analogous phospholipids.

| Lipid/surfactant (& headgroup) | Number of Carbons in tail group | Max $C_s^{-1}$/mN m$^{-1}$ | $A_{lim}$/Å$^2$ | $\pi_{col}$/mN m$^{-1}$ | $A_{col}$/Å$^2$ | Alkyl tail tilt angle (relative to the surface normal) |
|---|---|---|---|---|---|---|
| $C_{18}$Lyso-PC [48] | 18 | 61 | 70 | 41 | 33 | 75° (at 15 mN m$^{-1}$) |
| SB3-18 | 18 | 52 | 46 | 37 | 20 | 53° (at 15 mN m$^{-1}$) |
| DPPC [50,57] | 16 | 200 | 54 | 56 | 43 | 35° (at 15 mN m$^{-1}$) |
| SB3-18-2 | 18 | 184 | 48 | 54 | 38 | 8° (at 35 mN m$^{-1}$) |

great potential since these materials are far easier to synthesise at a fraction of the cost and time expense of their phospholipid counter-parts.

## Acknowledgements

The financial support in the form of a PhD studentship for GH from Diamond Light Source and the University of Bath is gratefully acknowledged. We would also like to thank Diamond and ISIS for awarded beamtime (Experiments SI9909 and RB1320376/RB1410545 respectively) and Diamond for the use of the BAM. Thanks are also extended to the I07 beamline, INTER beamline and SURF beamline staff for their assistance in collecting the XRR and NR data.

## Appendix A. Supplementary material

Supplementary data associated with this article can be found, in the online version, at http://dx.doi.org/10.1016/j.jcis.2016.04.020.

## References

[1] C. Reich, Surfactants in Cosmetics, second ed., Marcel Dekker, New York, 1997.
[2] C.M. Magin, S.P. Cooper, A.B. Brennan, Non-toxic antifouling properties, Mater. Today 13 (4) (2010) 36–44.
[3] A.B. Lowe, M. Vamvakaki, M.A. Wassal, et al., Well-defined sulfobetaine-based statistical copolymers as potential antibioadherent coatings, J. Biomed. Mater. Res. 52 (1) (2000) 88–94.
[4] Y. Yuan, F. Ai, X. Zang, et al., Polyurethane vascular catheter surface grafted with zwitterionic sulfobetaine monomer activated ozone, Colloids Surf., B 35 (1) (2004) 1–5.
[5] Z. Zhang, T. Chao, S. Chen, et al., Superlow fouling sulfobetaine and carboxybetaine polymers on glass slides, Langmuir 22 (4) (2006) 10072–10077.
[6] Z. Zhang, S. Chen, Y. Chang, et al., Surface grafted sulfobetaine polymers via atom transfer radical polymerisation as superlow fouling coatings, J. Phys. Chem. B 110 (2006) 10799–10804.
[7] J.T. Sun, Z.Q. Yu, C.Y. Hong, et al., Biocompatible zwitterionic sulfobetaine copolymer-coated mesoporous silica nanoparticles for temperature-responsive drug release, Macromol. Rapid Commun. 33 (9) (2012) 811–818.
[8] Q. Guangmiao, J. Cheng, J. Wei, et al., Synthesis, characterization and surface properties of series sulfobetaine surfactants, J. Surfactants Deterg. 14 (1) (2011) 31–35.
[9] G.A. Davis, P.G. Abend, W.M. Linfield, The synthesis and surface properties of certain amphoteric compounds, J. Am. Oil Chem. Soc. 40 (1963) 114–117.
[10] G. Maulucci, M. Spirito, G. Briganti, Particle size distributions in DMPC vesicle solutions undergoing different sonication times, Biophys. J. 88 (5) (2005) 3543–3550.
[11] D. Marsh, General features of phospholipid transitions, Chem. Phys. Lipids 57 (2) (1991) 109–120.
[12] D.M. Telesford, Langmuir Trough and Brewster Angle Microscopy Study of Model Lung Surfactant Monolayers at the Air/Aqueous Interface, Ohio State University, 2012.
[13] Y.A. Shchipunov, A.F. Kolpakov, Phospholipids at the oil/water interface: adsorption and interfacial phenomena in an electric field, Adv. Colloid Interface Sci. 35 (1991) 31–138.
[14] J.F. Nagle, S. Tristram-Nagle, Structure of lipid bilayers, Biochim. Biophys. Acta 1469 (2000) 159–195.
[15] M.C. Petty, Langmuir-Blodgett Films, Cambridge University Press, Cambridge, 1996.
[16] J. Liu, J.C. Conboy, Structure of a gel phase lipid bilayer prepared by the Langmuir-Blodgett/Langmuir Schaefer method characterized by sum-frequency vibrational spectroscopy, Langmuir 21 (20) (2005) 9091–9097.
[17] C. Venien-Bryan, P. Lenne, C. Zakri, et al., Characterization of growth of 2D protein crystals on a lipid monolayer by ellipsometry and rigidty measurements coupled to electron microscopy, Biophys. J. 74 (1998) 2649–2657.
[18] T.H. Lee, H. Mozsolitis, M.I. Aguilar, Measurement of the affinity of melittin for zwitterionic and anionic membranes using immobilized lipid biosensors, Chem. Biol. Drug Des. 58 (6) (2008) 464–476.
[19] M.C. Sin, S. Chen, Y. Chang, Hemocompatibility of zwitterionic interfaces and membranes, Polym. J. 46 (2014) 436–443.
[20] G. Ma, H.C. Allen, Condensing effect of palmitic acid on DPPC in mixed Langmuir monolayers, Langmuir 23 (2007) 589–597.
[21] K. Kewalramani, H. Hlaing, B.M. Ocko, et al., Effects of divalent cations on phase behaviour and structure of a zwitterionic phospholipid (DMPC) monolayer at the air-water interface, J. Phys. Chem. Lett. 1 (2010) 489–495.
[22] M. Ross, C. Steinem, H. Galla, et al., Visualization of chemical and physical properties of calcium-induced domains in DPPC/DPPS Langmuir-Blodgett layers, Langmuir 17 (8) (2001) 2437–2445.
[23] D. McLoughlin, R. Dias, B. Lindman, et al., Surface complexation of DNA with insoluble monolayers. Influence of divalent counterions, Langmuir 21 (2005) 1900–1907.
[24] D. Hönig, D. Möbius, Direct visualisation of monolayers at the air-water interface by brewster angle microscopy, J. Phys. Chem. 95 (12) (1991) 4590–4592.
[25] V. Vollhardt, Brewster angle microscopy: a preferential method for mesoscopic characterization of monolayers at the air/water interface, Curr. Opin. Colloid Interface Sci. 19 (3) (2014) 183–197.
[26] J.R. Lu, R.K. Thomas, J. Penfold, Surfactant layers at the air/water interface: structure and composition, Adv. Colloid Interface Sci. 84 (1–3) (2000) 143–304.
[27] X.-L. Zhou, S.-H. Chen, Theoretical foundation of X-ray and neutron reflectometry, Phys. Rep. 257 (4–5) (1995) 223–348.
[28] J.A. Dura, C.F. Richter, C.F. Majkrzak, et al., Neutron reflectometry, X-ray reflectometry and spectroscopic ellipsometric characterisation of thin $SiO_2$ on Si, Appl. Phys. Lett. 73 (1998) 2131.
[29] V.F. Sears, Neutron scattering lengths and cross sections, Neutron News 3 (3) (1992) 26–37.
[30] J.D. Hines, G. Fragneto, R.K. Thomas, et al., Neutron reflection from mixtures of sodium dodecyl sulfate and dodecyl betaine adsorbed at the hydrophobic solid/aqueous interface, J. Colloid Interface Sci. 189 (1997) 259–267.
[31] J. Penfold, R.M. Richardson, A. Zarbakhsh, et al., Recent advances in the study of chemical surfaces and interfaces by specular neutron reflection, J. Chem. Soc., Faraday Trans. 93 (22) (1997) 3899–3917.
[32] J.R. Lu, E.A. Simister, R.K. Thomas, Structure of an octadecyltrimethylammonium bromide layer at the air/water interface determined by neutron reflection: systematic errors in reflectivity measurements, J. Phys. Chem. 97 (1993) 6024–6033.
[33] J. Daillant, E. Bellet-Amalric, A. Braslau, et al., Structure and fluctuations of a single floating lipid bilayer, Proc. Natl. Acad. Sci. 102 (33) (2005) 11639–11644.
[34] P.S. Pershan, M.L. Schlossman, Liquid Surfaces and Interfaces: Synchrotron X-ray Methods, Cambridge University Press, Cambridge, 2012.
[35] L.A. Clifton, M.W.A. Skoda, E.L. Daulton, et al., Asymmetric phospholipid: lipopolysaccharide bilayers; a Gram negative bacterial outer membrane mimic, Interface 10 (2013).
[36] C.R. Hatty, A.P. Le Brun, V. Lake, et al., Investigating the interactions of the 18 kDa translocator protein and its ligand PK11195 in planar lipid bilayers, Biochim. et Biophys. Acta-Biomembranes 1838 (3) (2014) 1019–1030.
[37] T. Arnold, C. Nicklin, J. Rawle, et al., Implementation of a beam deflection system for studies of liquid interfaces on beamline I07 at Diamond, J. Synchrotron Radiat. 19 (2012) 408–416.
[38] A. Gibaud, G. Vignaud, The correction of geometrical factors in the analysis of X-ray reflectivity, Acta Crystallogr. A 49 (1993) 642–648.
[39] X.L. Zhou, S.W. Chen, Theoretical foundation of X-ray and neutron reflectometry, Phys. Rep. 257 (4–5) (1995) 223–348.
[40] J. Webster, S. Holt, Dalgliesh. INTER the chemical interfaces reflectometer on target station 2 at ISIS, Phys. B 385 (2006) 1164–1166.
[41] D.G. Bucknall, J. Penfold, J.R.P. Webster, A. Zarbakhsh, R.M. Richardson, A. Rennie, J.S. Higgins, R.A.L. Jones, P. Fletcher, R.K. Thomas, S. Roser, E. Dickinson, SURF – a second generation neutron reflectometer, Proceedings of the Meetings ICANS-XIII and ESS-PM4, vol. 27 (18), 1995, pp. 123–129.
[42] A. Nelson, Co-refinement of multiple-contrast neutron/X-ray reflectivity data using MOTOFIT, J. Appl. Crystallogr. 39 (2) (2006) 273–276.
[43] F. Abeles, Investigations on the propagation of sinusoidal electromagnetic waves in stratified media: application to thin films, Ann. Phys. 3 (1948) 504–520.
[44] O. Heavens, Optical Properties of Thin Films, Butterworth, London, 1955.
[45] N.J. Hardy, T.H. Richardson, F. FGrunfeld, Minimising monolayer collapse on Langmuir troughs, Colloids Surf. A: Physicochem. Eng. Aspects 284-285 (2006) 202–206.
[46] T. Reis, Introduction a la Chimie-Physique des Surfaces, Dunod, Paris, 1952.
[47] W.D. Harkins, The Physical Chemistry of Surface Films, Reinhold, New York, 1952.
[48] M. Flasinski, P. Wydro, M. Broniatowski, Lyso-phosphatidylcholines in Langmuir monolayers-influence of chain length on physicochemical characteristics of single-chained lipids, J. Colloid Interface Sci. 418 (2014) 20–30.
[49] J.T. Davies, E.K. Rideal, Interfacial Phenomena, Reinhold, New York, 1963.
[50] S.L. Duncan, R.G. Larson, Comparing experimental and simulated pressure-area isotherms for DPPC, Biophys. J. 94 (2008) 2965–2986.
[51] G. Espinosa, I. Montero-Lopez, F. Monroy, et al., Shear rheology of lipid monolayers and insights on membrane fluidity, Proc. Natl. Acad. Sci. 108 (15) (2010) 6008–6013.
[52] I.R. Gomez-Serranillos, J. Minones, P. Dynarowicz-Latka, et al., Study of pi-A isotherms of miltefosine monolayers spread at the air/water interface, Phys. Chem. Chem. Phys. 6 (2004) 1580–1586.
[53] M. Flasinski, M. Broniatowski, P. Wydro, et al., Comparative characteristics of membrane-active single-chained ether phospholipids: PAF and Lyso-PAF in Langmuir monolayers, J. Phys. Chem. B 116 (2012) 3155–3163.
[54] C.R. Flach, J.W. Brauner, R. Mendelsohn, Calcium ion interactions with insoluble phospholipid monolayer films at the A/W interface. External reflection-adsorption IR studies, Biophys. J. 65 (1993) 1994–2001.

[55] M. Sovago, G.W.H. Wurpel, M. Smits, M. Müller, M. Bonn, Calcium-induced phospholipid ordering depends on surface pressure, J. Am. Chem. Soc. 129 (2007) 11079–11084.
[56] A. Osak, P. Dynarowicz-Latka, O. Conde, et al., Edelfosine – a new antineoplastic drug based on a phospholipid like structure: the Langmuir monolayer study, Colloids Surf. A: Physicochem. Eng. Aspects 2008 (319) (2008) 71–76.
[57] A.L. Aroti, E. Maltseva, G. Brezesinski, Effects of hofmeister anions on DPPC langmuir monolayers at the air-water interface, J. Phys. Chem. B 108 (2004) 15238–15245.
[58] C.W. McConlogue, T.K. Vanderlick, A close look at domain formation in DPPC monolayers, Langmuir 13 (1997) 7158–7164.
[59] H. Mohwald, From Langmuir monolayers to nanocapsules, Colloids Surf. A: Physicochem. Eng. Aspects 171 (1–3) (2000) 25–31.
[60] J.A. Holdaway, A Study of the Structure and Formation of Biocompatible Mesostructured Polymer-Surfactant Hydrogel Films, University of Bath, 2014.
[61] E.G. Tveten, X-ray and Neutron Reflectivity Studies of Nanodiscs Below the Air-Water Interface, University of Copenhagen, 2011.
[62] H. Mohwald, Handbook for Biological Physics, Elsevier Science B.V, 1995.
[63] D. Vaknin, K. Kjaer, J. Als-Nielsen, et al., Structural properties of phosphatidylcholine in a monolayer at the air/water interface, Biophys. J. 59 (1991) 1325–1332.
[64] V.M. Kaganer, H. Möhwald, P. Dutta, Structure and phase transitions in Langmuir monolayers, Rev. Modern Phys. 71 (3) (1999) 779–819.
[65] M. Wadsater, R. Barker, K. Mortensen, et al., Effect of phospholipid composition and phase on nanodisc films at the solid-liquid interface as studied by neutron reflectivity, Langmuir 13 (29) (2013) 2871–2880.